Journal of Visualization, Vol. 12, No. 4 (2009) 383-391

Regular Paper

Visualization of Flow Past a Square Prism with Cut-Corners at the Front-Edge

Ueda, Y.*[1], Kurata, M.*[2], Kida, T.*[3] and Iguchi, M.*[1]

*1 Division of Materials Science and Engineering, Graduate School of Engineering, Hokkaido University, Nishi 8, Kita 13, Kita-Ku, Sapporo, Hokkaido 060-8628, Japan. E-mail: y-ueda@eng.hokudai.ac.jp
*2 Department of Mechanical Engineering, College of Engineering, Setsunan University, 17-8, Ikedanaka-Machi, Neyagawa, Osaka 572-8508, Japan.
*3 Professor Emeritus, Division of Mechanical Engineering, Graduate School of Engineering, Osaka Prefecture University, 1-1, Gakuen-Cho, Naka-Ku, Sakai, Osaka 599-8531, Japan.

Received 14 July 2008
Revised 3 April 2009

Abstract : Flow past a square prism with cut-corners at the front-edge is numerically and experimentally visualized to investigate a mechanism of drag reduction. An adaptive numerical scheme based on the vortex method is implemented for two values of the Reynolds number between 200 and 1,250, and the results are compared with experiments. Experimental visualization techniques include the hydrogen-bubble technique at $Re = 4,000$ and the oil-flow technique at $Re = 10,000$ for a global wake formation, and the aluminum-flake technique for transient flow at the early stage of motion at $Re = 1,250$. A similar reattachment flow pattern is shown in a wide range of the Reynolds number between 200 and 10,000, which implies a possibility of the drag reduction in the Reynolds number being approximately lower than 8,000 unlike the previous findings.

Keywords : Drag Reduction, Square Prism, Vortex Method, Hydrogen-Bubble Technique, Aluminum-Flake Technique, Oil-Flow Technique.

1. Introduction

A strong von Kármán vortex street could affect a vibration of a structure and so it is also desirable to decrease the strength of a wake vorticity. Flow past a cylinder with cut-corners at the front-edge is an intriguing issue in the study of drag reduction and suppression of the vibration. Among a few studies about the drag reduction on a rectangular cylinder with cut-corners (see, for instance, Kurata *et al.* 1998, 1999, 2008; Igarashi *et al.* 2005), the drag reduction is known to be achieved under a certain cutout dimension in which the separated turbulent shear layer from the corner C or D reattaches to the surface A-H or F-G (see Fig.1). Prior studies have made the experimental flow visualization to investigate an overall view on the wake flow pattern due to the cut-corners. A further overview about a series of earlier studies on the drag reduction is presented in the associated article of Kurata *et al.* (2008).

This paper aims to investigate the reattachment point of the separated shear layer and its effect on the drag reduction. Visualization techniques include the two-dimensional vortex particle method (see Ueda *et al.* 2005) as a computation and the aluminum-flake technique for a lower range

of the Reynolds number, the hydrogen-bubble technique for the moderately high Reynolds number and the oil-flow technique for the high Reynolds number. Validity of the present vortex method for resolution is also verified in §§4.1 against the aluminum-flake visualization about transient flow past an impulsively started square prism with 25% cut-corners at the early stage of motion. A pseudo-steady flow is then investigated in §§4.2 for a wide range of the Reynolds number by employing various approaches: the vortex method for $Re = 200$; the hydrogen-bubble technique for $Re = 4,000$; the oil-flow technique for $Re = 10,000$. In particular, the reattachment point of the separated shear flow on the side surface of the prism is visualized by the vortex method and the oil-flow technique. Finally, a free-streamline model which is proposed by observation of the present flow visualizations supports the experimental results about the optimal dimension of the cutout for the drag reduction.

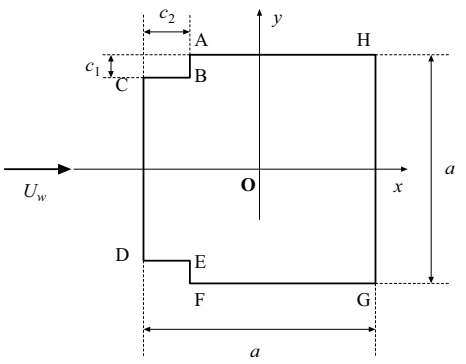

Fig.1. Notations for a square prism with cut-corners at the front-edge immersed in a uniform flow U_w.

2. Governing Equations and Vortex Particle Method

2.1. Two-Dimensional Navier-Stokes Equations

We look at the unsteady incompressible viscous flow about a square prism, Σ, with cut-corners at the front edge (see Fig.1). The prism Σ has center $\mathbf{O}$, boundary $\partial\Sigma$, and breadth a. At $t \to +0$ the prism is impulsively immersed in a constant flow $U_w \boldsymbol{e}_x$ with $U_w > 0$. The time t_o is nondimensionalized based on a as $t := U_w t_o / a$. The liquid has kinematic viscosity ν. The resulting flow with typical Reynolds number $Re = U_w a / \nu$ has velocity and vorticity fields $\boldsymbol{u}(\boldsymbol{x}, t)$ and $\omega(\boldsymbol{x}, t)\boldsymbol{e}_z$ such that $\boldsymbol{u}(\boldsymbol{x}, 0) = \mathbf{0}$ and, for $t > 0$,

$$\frac{\partial \omega}{\partial t} + \boldsymbol{u} \cdot \nabla \omega = \frac{1}{Re} \nabla^2 \omega \quad \text{in } \mathbb{R}^2 \setminus \Sigma, \tag{1}$$

with the no-slip boundary condition $\boldsymbol{u}(\boldsymbol{x}, t) = \mathbf{0}$ on $\partial\Sigma$, and $\boldsymbol{u}(\boldsymbol{x}, t) \to \boldsymbol{\nabla}\Phi H(t)$ and $\oint_{\mathscr{C}_r} \boldsymbol{u} \cdot \mathrm{d}\boldsymbol{\ell} \to 0$ as $|\boldsymbol{x}| \to \infty$ where $\mathscr{C}_r = \{\boldsymbol{x} \mid |\boldsymbol{x}| = r\}$ and H denotes the usual Heaviside step function. In addition, Φ is a scalar function which satisfies $\nabla^2 \Phi = 0$ in a solenoidal field.

2.2. Vortex Particle Method

Using the Lagrangian formulation, the vorticity transport equation (1) is split into the Euler equation and the viscous diffusion equation. The convective and diffusion steps are separately handled by a panel method and the Particle Strength Exchange (PSE) method (see Degond & Mas-Gallic 1989). The vortex method is based on the spatial discretization of the vorticity field which consists of Lagrangian particles. The discretized vorticity field can be written in the numerical quadrature which is represented by vortex particles. The location of the scattered vortex particles with a finite core size is regularized by a vorticity distribution function called the cutoff function. In this computation, the Gaussian distribution function is employed. The velocity field $\boldsymbol{u}$ at $\boldsymbol{x}$ is calculated by the Biot-Savart law which spends $O(N^2)$ computational cost. The Fast Multipole Method (FMM) of Greengard & Rokhlin (1987) decreases to $O(N)$ iterations. After the vortex particles travel, there is a non-zero slip velocity on the surface of the body which is induced by all vortex particles and the uniform velocity. The no-slip boundary condition is then enforced by using a vortex sheet on $\partial\Sigma$ whose strength obeys the boundary integral equation. The vortex sheet created is diffused into the vortex particle in the fluid as $\nu(\partial\omega/\partial\boldsymbol{n}) = -(\partial/\partial t)(\boldsymbol{u} \cdot \boldsymbol{s})$ on $\partial\Sigma \times [0, t]$. The

convergence of the vortex method with a finite core radius is obtained under the condition of particle overlapping at any time. Furthermore, the accuracy of the vortex method relies on the evaluation of the volume (or area for 2D) of the scattered vortex particles (see Ueda & Kida 2008). This truncation error is straightforwardly removed by remeshing after a few time steps (see Cottet & Koumoutsakos 2000). In addition, the vortex particle simulation without the remeshing is given in Noda *et al.* (2003) for a square prism with 25% cut-corners.

3. Experimental Visualization Procedure

Experimental visualization techniques include the aluminum-flake technique for the transient local flow near the prism, the hydrogen-bubble technique and the oil-flow technique for the wake formation behind the prism. In particular, the reattachment point on the side surface of the prism is investigated by the oil-flow visualization.

In the aluminum-flake technique, a particulate such as aluminum flake was placed in the water tank of 1,200 (mm) long, 400 (mm) wide and 400 (mm) deep. The experimental set-up consisted of the water tank, a pair of halogen lamps, the CCD camera, the experimental model and the moving device of the square prism. The square prism with 25% cut-corners ($c_1/a = c_2/a = 0.25$), immersed in the water tank, was 374 (mm) long in the spanwise direction and it was sustained on the mount table. A clearance between the end-surface of the prism and the sidewall of the tank was 0.5 (mm). At $t = 0$ the square prism abruptly moved with the constant speed of 25 (mm/s). The Reynolds number was then calculated as $Re = 1,250$. The instantaneous flow was visualized by the CCD camera exposing over 1/4 (s) with F2.8 and ISO400. The CCD camera was fixed with the mount table to move in parallel with the prism. The horizontal cross-section, about 30 (mm) apart from the sidewall of the water tank, of the flow was illuminated by a pair of halogen lamps which were set on the front and back surfaces of the water tank for the photograph. In addition, the slit width of the halogen lamp was 2.0 (mm).

In the hydrogen-bubble technique, a square prism with the breadth of 30 (mm) was immersed in the open-type towing water tank of 2,000 (mm) long, 400 (mm) wide and 400 (mm) deep, and the prism and a kink-shaped tungsten wire with a diameter of 0.1 (mm) which was set at 60 (mm) ahead of the center of the prism were both fixed on the moving device. The wake flow behind the prism was illuminated by a pair of halogen lamps. The calculated Reynolds number was also 4,000.

In the oil-flow technique, a square prism with the breadth of 30 (mm) was immersed in the open-type wind tunnel whose cross-section was 380 (mm) $\times$ 380 (mm). The maximum wind velocity was 40 (m/s) and the turbulence intensity of the wind tunnel was a little larger than 1%. The square prism was set, in the uniform flow direction, inside the sidewall consisting of two parallel plates with the distance of 360 (mm). The white oil film which was combined with oxidized titanium and olefin acid was applied on the surface of the prism. The calculated Reynolds number was 10,000.

4. Results and Discussion

4.1. Transient Flow Past an Impulsively Started Square Prism with 25% Cut-Corners at the Early Stage of Motion

We first examine a transient flow past a square prism with $c_1/a = c_2/a = 0.25$, which abruptly moves with a constant speed U_w. This case makes it possible to verify the accuracy of the employed vortex particle simulation against the aluminum-flake visualization. The parameters of the simulation employed are $\Delta t = 0.01$ and $M = 800$ panels. Initially, 57,032 particles of the core radius, $\epsilon = 4.0 \times 10^{-3}$, are located in the vicinity of the square prism.

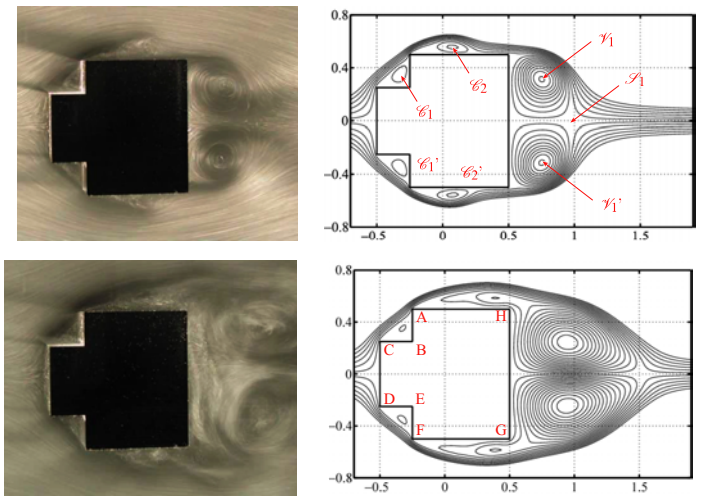

Fig.2. Transient flow past a square prism with 25% cut-corners at $Re = 1,250$ and (top) $t = 1.5$; (bottom) $t = 4.5$. (Left): experimental photographs of the aluminum-flake technique; (Right): computed streamlines.

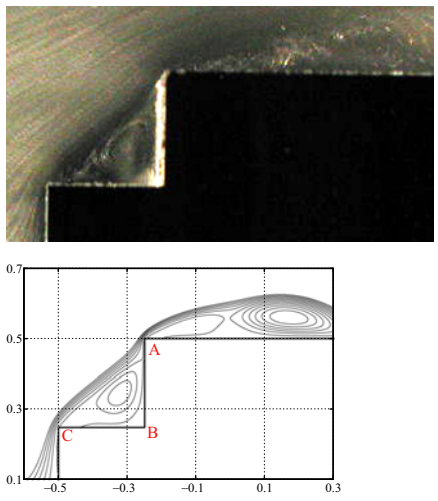

Fig.3. Magnified view of the separated shear layer near the upper cut-corner at $Re = 1,250$ and $t = 2.0$. (Top): experimental photograph; (Bottom): computed streamline.

In Fig.2 selected comparisons of computed and experimental instantaneous flow patterns are presented for $Re = 1,250$ and at $t = 1.5$ and 4.5. According to Nozu & Tamura (1997), a transition of the separated shear layer produces fine-scale three-dimensionalities in the $Re = 1,000$ flow past a square prism without a cut-corner. When a square prism abruptly starts with $Re = 10,000$ a distinct discrepancy of the spanwise correlation of the time history of the pressure is computationally measured to appear at about $t = 140$ and experimentally measured at $t \approx 10.20$ after the movement (see Tamura *et al.* 1998). The appearance of the three-dimensionality is as well for a circular cylinder (see Williamson 1996) and the saturation of the transverse enstrophy computationally appears at about $t = 150$ after the impulsive movement at $Re = 300$ (see Cottet & Poncet 2003). Following these findings, the present transient flow of Fig.2 is found to behave like two-dimensional shedding mode and it can be compared with the 2D computation. In Fig.2 it may be seen that the computation is nicely identical with the experimental flow visualization. At $t = 1.5$ a pair of the circulation flow are observed in the cutout region ($\mathscr{C}_1$ and $\mathscr{C}_1'$) and the upper/down side surface of the prism ($\mathscr{C}_2$ or $\mathscr{C}_2'$). The twin vortex is formed behind the prism ($\mathscr{V}_1$ and $\mathscr{V}_1'$) and the saddle point ($\mathscr{S}_1$) appears at the end of the wake. As seen in the streamlines, the position of $\mathscr{C}_2$ moves downward near the corner H and the distinct circulation disappears with increasing of time. The twin vortex grows and the saddle point $\mathscr{S}_1$ moves downstream.

Figure 3 shows a comparison of the initial flow near the cut-corner between the experiment and computation. In the magnified view, the closed streamline is observed in the cutout region and the weak secondary circulation is formed due to the separated flow at the corner A. The computed positions of $\mathscr{C}_1$ and $\mathscr{C}_2$ are virtually in good agreement with the experimental photograph.

4.2. Reattachment Position and Wake Behavior Due to a Separated Shear Layer

As mentioned in Introduction, a reattachment of a separated shear layer from the front-corner plays an important role to decrease the drag force. This section visualize a pseudo-steady flow around the square prism, having three kinds of the cutout dimensions, to investigate the effect of the vortex shedding from the front-corner on the wake formation behind the prism. The following three kinds of cutout dimensions are selected: (i) $c_1/a = c_2/a = 0.00$; (ii) $c_1/a = c_2/a = 0.25$; (iii) $c_1/a = 0.10, c_2/a = 0.20$. The selected Reynolds numbers are at 200 for the computation, 4,000 for the hydrogen-bubble technique and 10,000 for the oil-flow technique. The experimental and computational conditions are shown in Fig.8. For reference the contour map of the drag coefficient

with respect to the cutout dimension which was experimentally measured by a force transducer is reproduced in Fig.4 (see Kurata *et al.* 2008). One can find that the optimal dimension of the cutout is (iii).

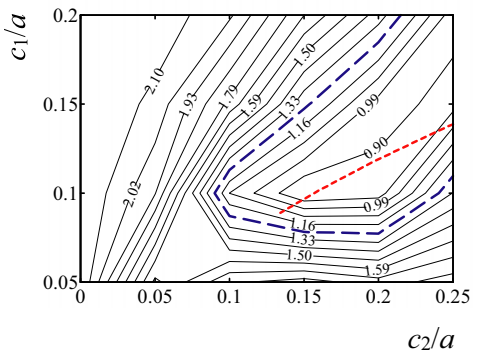

Fig.4. Contour map of C_D with respect to the cutout dimension for the square prism (see Kurata *et al.* 2008). Dotted line indicates the optimal dimension which is obtained from the free-streamline theory of Eq.(4), and dashed line indicates the value of C_D^* for a circular cylinder.

Figure 5 shows the computed streamline near the cut-corner at $Re = 200$ and the oil-film on the side surface of the prism (C-B and A-H) due to the separated shear flow at $Re = 10,000$. According to the knowledge of Williamson (1996), the low Reynolds number flow being less than 190 past a circular cylinder behaves like a two-dimensional shedding mode and the present 2D computation is almost reasonably compared with the experiments. In (i) of Fig.5 the backflow is observed on the side surface of the prism where the oil film seems not to be parallel to the surface A-H. We here notice an experimental drawback that the oil flow has a tendency to grow down slightly due to the gravity because of the vertical set of the experimental model in the wind tunnel. The photograph of (i) shows that the three-dimensional structures develop in the backflow which changes in the spanwise direction. The observation of the three-dimensionality is found to make sense for Williamson (1996) who reviews the three-dimensional vortex dynamics in a circular cylinder wake. In (ii), the separated shear layer from the corner C seems to reattach to the surface A-B and separate again from the corner A. The backflow, in a similar to (i), occurs on the surface A-H due to the second separation so that the reattachment is not observed on the surface A-H. In (iii), the separated shear flow from the corner C seems to reattach close behind the corner A (obviously judged from the photograph) and smoothly advect, although being so weak, along the surface A-H. Note that there is no backflow region (obviously judged from the CFD result). Further observation of (iii) is that the local flow inside the

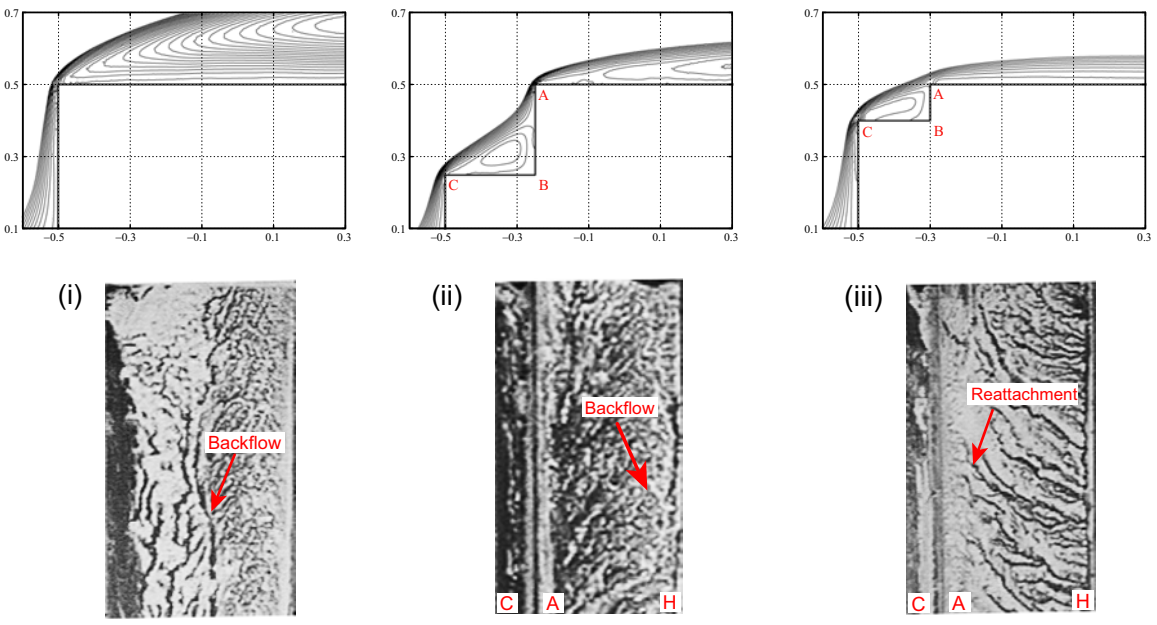

Fig.5. Comparison of the separated shear layer between (i): $c_1/a = c_2/a = 0.00$, (ii): $c_1/a = c_2/a = 0.25$ and (iii): $c_1/a = 0.10, c_2/a = 0.20$. (Top): computation at $Re = 200$ and $t = 150$; (Bottom) oil flow on the surface C-B and A-H at $Re = 10,000$.

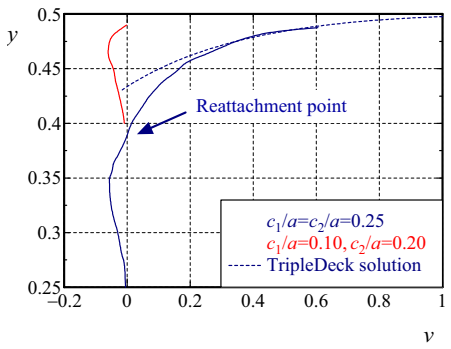

Fig.6. Comparison of the y-component of the velocity on $x = -0.01$ upstream from the surface A-B.

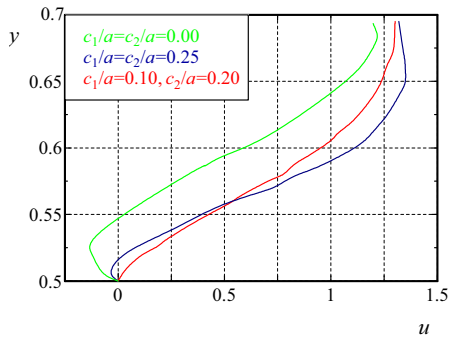

Fig.7. Comparison of the x-component of the velocity at $x = 0.1$ downstream from the corner A.

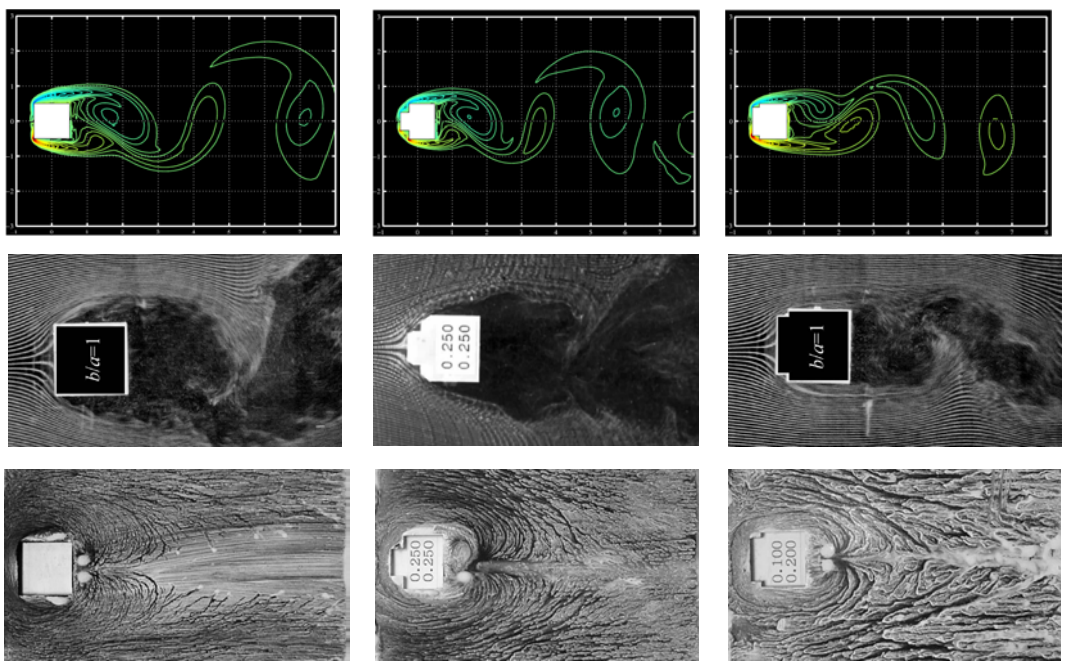

Fig.8. Visualizations of wake flow pattern; (top): computed iso-vorticity line at $Re = 200$ and $t = 150$; (middle): experimental photograph of hydrogen-bubble technique at $Re = 4,000$; (bottom): experimental photograph of oil-flow technique at $Re = 10,000$. (Left): $c_1/a = c_2/a = 0.00$; (Center): $c_1/a = c_2/a = 0.25$; (Right): $c_1/a = 0.10, c_2/a = 0.20$.

cutout is almost a cavity flow. The reattachment is thought to make the drag fore reduced in (iii). From the observation of Fig.5, all kinds of flow patterns (i) to (iii), with the exception of the three-dimensionality, seem to be similar in Re although the wide variation in Re between 200 and 10,000 changes the separated shear layer from a laminar to a turbulent one.

Indeed, Fig.6 or 7 shows the computed y- (or x-) component of the velocity on the vicinity of the surface A-B (or close behind the corner A). In Fig.6 the separated shear flow from the corner C seems to reattach on the surface A-B around $y \approx 0.39$ in (ii) although there is no reattachment in (iii). This results in that there is no backflow on the surface A-H in (iii), as shown in Fig.7, and the separated shear layer smoothly advects along the surface.

The high Reynolds number analysis near a sharp corner describes a separated flow on the basis of the Triple-Deck theory. As explained in Sychev *et al.* (1998), one needs to distinguish a lot of local domains near the corner. In this study, we select the domain (2), cited from Sychev *et al.* (1998), which governs the main deck of the boundary-layer, $O(Re^{-4/9})$ in the tangential direction and

$O(Re^{-1/2})$ in the normal direction, ahead of the corner A. In domain (2) the tangential velocity u_s along the surface is written as, in the curvilinear coordinates, $\hat{x}$, $\hat{y}$, referred to the body surface $\hat{y}=0$ in the streamwise direction with the origin set at the corner,

$$u_s(\hat{x},\eta) \approx (4k^2)^{1/4} Re^{1/2} (-\hat{x})^{1/4} \left[\frac{5}{3} A_0 \eta^{2/3} + \frac{2}{3} B_0 \eta^{-1/3} + \frac{3}{5A_0} \eta^{-2/3} \right], \tag{2}$$

where $\eta := (k/2)^{1/4} \left[Y/(-\hat{x})^{3/8} \right]$ and $Y := Re^{1/2}\hat{y}$. In addition, $A_0 = 1.9507$ and $B_0 = -1.5776$. The asymptotic solution of Eq.(2) is depicted in Fig.6 as a dotted line. This vortex particle method is found to be in nice resolution for an intricate shear flow in the vicinity of a separation point.

Figure 8 shows the wake flow patterns in the pseudo-steady regime for a wide range of Re. The oil-flow technique is inadequate to visualize a fine structure of the wake, unlike the hydrogen-bubble one, and it is rather suited to capture a macroscopic structure. As shown in Figs.5, 6 and 7, the reattachment in (iii) makes the separated shear flow smoothly advect along the surface A-H. This could decrease the strength of a von Kármán vortex street and the width of two parallel vortex streets becomes narrow, as shown in Fig.8. A solid body experiences the drag force, in a viscous fluid, which is described as

$$D = -\rho \int_{\mathbb{R}^2 \setminus \Sigma} y \frac{\mathrm{d}\omega}{\mathrm{d}t} \, \mathrm{d}S - \rho \int_{\mathbb{R}^2 \setminus \Sigma} v\omega \, \mathrm{d}S, \tag{3}$$

where $\boldsymbol{u} = (u, v)$ and S is the surface of the body. Equation (3) is easily obtained by employing Green's theorem to the Navier-Stokes equations. The narrow wake width due to the cutout makes the first term of Eq.(3) be small and the weak strength makes the second term be sufficiently small as well. In Fig.8, the wake width is observed to be narrow in the optimal cutout and the drag reduction could be achieved even in a lower range of Re being less than the threshold Reynolds number of $Re_t \approx 8,000$ under which transition behavior of a separated shear layer changes from a laminar to a turbulent separation.

5. Free-Streamline Model

The drag reduction seems to be achieved when the separated flow, at the corners A and C or D and F, is along the side surfaces, A-H and F-G. The optimal case is that; the streamline of the separated flow at the corner C and D reattaches around the corner A and F and then the streamline is smoothly along the surface A-H and F-G. In this case the pressure inside the cutout region is thought to be almost constant (see the Triple-Deck theory of Sychev 1998). Following the physical insight, this section establishes a simple physical model, based on the free-streamline theory, to predict an optimal dimension of the rectangular-shaped cutout.

Figure 9 shows a physical plane of the free-streamline model. The uniform flow is incoming to the front surface C-D and splits into S-C and S-D and then separation occurs at the corners C and D. The velocity of the separated flow is so large that the viscous effect might be neglected. This fact enables one to regard the separated streamline as the *free-streamline*. Here, the magnitude of the velocity on the separated streamline at the corner C or D is constant and, therefore, the velocity, q_c, is normalized by the uniform velocity $U_w = 1$. After the separation at the corners C and D, the streamline attaches to the upper and bottom surfaces A and F and, then, flows downstream along the surface A-H_∞ and F-G_∞. The assumption of the potential flow allows one to use the complex velocity potential, $f = \phi + i\psi$, due to the singularity. Here, ϕ is the velocity potential and ψ is the stream function. Then, the complex velocity potential, $F(w) = f(w) + \bar{f}(q_c^2/\bar{w})$ ($F(w)$ is obtained by using the Milne-Thomson circle theorem for which one can refer to the textbook of Batchelor 1967 or Milne-Thomson 1968), is written as, taking into account that doublets placed at A, F and H_∞, G_∞, $F(w) = 2\mu/(w^2-1) - 2\mu w^2/(w^2 - q_c^4)$, where w is the complex velocity which is expressed by $w = u - iv$, and the strength of the doublet, μ, is a constant. Because of $w = (\mathrm{d}F/\mathrm{d}w)(\mathrm{d}w/\mathrm{d}z)$, the above complex velocity potential gives $\mathrm{d}z/\mathrm{d}w = -4\mu/(w^2-1)^2 + 4\mu q_c^4/(w^2 - q_c^4)^2$. Integrating this

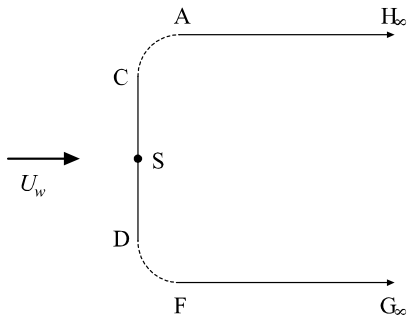

Fig.9. Physical plane of the free-streamline model.

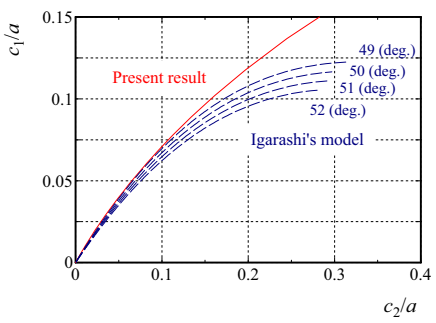

Fig.10. Appropriate dimensions of the cutout shape.

equation, we have

$$\frac{\Delta x}{4\mu q_c} = \frac{1+q_c^2}{2q_c^2(q_c^2-1)} + \frac{q_c^2-1}{4q_c^3}\log\left(\frac{q_c-1}{q_c+1}\right), \qquad \frac{\Delta y}{4\mu q_c} = \frac{q_c^2+1}{4q_c^3}\tan^{-1}\left(\frac{2q_c}{q_c^2-1}\right) - \frac{q_c^2-1}{2q_c^2(q_c^2+1)}, \tag{4}$$

where $\Delta x := c_2/a$, $\Delta y := c_1/a$ and $\mu = a/(2\pi)$. Figure 10 shows the result of Eq.(4) together with the earlier geometrically-based prediction of Igarashi *et al.* (2005). It is found that the prediction of Igarashi *et al.* (2005), which is modelized by matching the turbulent separation point of the circular cylinder to the cut-corners, is not similar to Eq.(4) in a large cutout dimension. Equation (4) is depicted in Fig.4 to verify this free-streamline model. In Fig.4, Eq.(4) passes through the region where the drag coefficient is minimum and this free-streamline model is thus thought to be valid for a wide range of the cutout dimension.

6. Conclusions

Drag reduction of a square prism with cut-corners has been investigated with some kinds of flow visualization technique for a wide range of the Reynolds number. Visualization techniques include a grid-based vortex method and the aluminum-flake technique for $Re = 200$ and $Re = 1,250$, the hydrogen-bubble technique for $Re = 4,000$ and the oil-flow technique for $Re = 10,000$. Primary results are summarized as follows:

- The transient flow past an impulsively started square prism with 25% cut-corners at the early stage of motion has been computed and verified against the aluminum-flake visualization.
- In the cutout shape of $c_1/a = 0.10, c_2/a = 0.20$, the separated shear layer reattaches on the side surface of the prism and then smoothly advects downstream. This makes the width of a von Kármán vortex alley be narrow and the strong drag reduction could be achieved.
- The present vortex method nicely resolves an intricate shear flow in the vicinity of a separation point against the Triple-Deck solution.
- The proposed model, based on the free-streamline theory, determines an optimal cutout dimension on the drag reduction.

References

Batchelor, G.K., An Introduction to Fluid Dynamics, (1967), Cambridge University Press.
Cottet, G.-H. and Koumoutsakos, P.D., Vortex Methods: Theory and Practice, (2000), Cambridge University Press.
Cottet, G.-H. and Poncet, P., Advances in direct numerical simulations of 3D wall-bounded flows by Vortex-in-Cell methods, *J. Comput. Phys.*, **193**, (2003), 136-158.
Degond, P. and Mas-Gallic, S., The Weighted Particle Method for Convection-Diffusion Equations, Part 1: The Case of an Isotropic Viscosity, Part 2: The Anisotropic Case, *Math. Comput.*, **53**, (1989), 485-525.
Greengard, L. and Rokhlin, V., A Fast Algorithm for Particle Simulations, *J. Comput. Phys.*, **73**, (1987), 325-348.
Igarashi, T., Muranaka, N. and Nakamura, H., Drag Reduction of a Rectangular Cylinder with Small Rectangular Cutout at Its Edges Normal to Air-Stream, *Annu. Conf. Japan Society of Fluid Mechanics*, (2005), No. AM05-04-016.
Kurata, M., Morisawa, T., Hirakawa, K., Yasutomi, Z. and Kida, T., Drag Reduction of a Bluff Body with Small Cutout at Its Edges (Case of Prism with Square Cross Section), *Trans. of JSME*, **64**- 618, B (1998), 397-404.

Kurata, M., Hirakawa, K., Yasutomi, Z. and Kida, T., Effect of Cutout at Front Edges to Drag Reduction of Square Prism, *Trans. Japan Aeronautical and Space Science*, **47**- 543, (1999), 174-181.
Kurata, M., Hirakawa, K., Yasutomi, Z. and Kida, T., Relationship between Near Wake and Drag Reduction of Square Prism Due to Cutout at Front Edges, *Trans. Japan Aeronautical and Space Science*, **47**- 550, (1999), 403-410.
Kurata, M., Ueda, Y., Kida, T. and Iguchi, M., Drag reduction due to cut-corners at the front-edge of a rectangular cylinder with the length-to-breadth ratio being less than or equal to unity, *ASME, J. Fluids Eng.*, **131**, (2009), 064501.
Milne-Thomson, L.M., Theoretical Hydrodynamics, (1968), Palgrave Macmillan.
Noda, K., Ueda, Y., Kida, T., Kurata, M., Yasutomi, Z. and Tamano, H., Transient Flow around an Impulsively Started Rectangular Cylinder by a Vortex Method (Effect of Cut-out of Front Edges), *Trans. of JSME*, **69**- 677, B (2003), 53-60.
Nozu, T. and Tamura, T., Application of computational fluid technique with high accuracy and conservation property to the wind resistant problems of buildings and structures. Part 1 Estimations of numerical errors of the interpolation method and its accuracy for the prediction of flows around a rectangular cylinder at low Reynolds numbers, *J. Struct. Constr. Eng.*, AIJ, **494**, (1997), 43-49.
Okajima, A., Ueno, H. and Abe, A., Influence of Reynolds number on flow and aerodynamic characteristics of bluff bodies with rectangular section of cut corners, *J. Wind Eng.*, **49**, (1991), 1-13.
Sychev, V.V., Ruban, A.I., Sychev, V.V. and Korolev, G.L., Asymptotic Theory of Separated Flows, (1998), Chap.2, Cambridge University Press.
Tamura, T., Miyagi, T. and Kitagishi, T., Numerical prediction of unsteady pressures on a square cylinder with various corner shapes, *J. Wind Eng. Ind. Aerodyn.*, **74**- 76, (1998), 531-542.
Ueda, Y. and Kida, T., Removal of spatial error due to distorted vortex particle location, *Private Communication*, (2008).
Ueda, Y., Sellier, A. and Kida, T., Analysis of unsteady interactions between cylinders by a Vortex Method, *Proc. ICVFM*, (2005), CD-ROM.
Williamson, C.H.K., Vortex dynamics in the cylinder wake, *Ann. Rev. Fluid Mech.*, **28,** (1996), 477-539.

Author Profile

Yoshiaki Ueda: He received his Ph.D. in 2003 from Department of Mechanical Engineering at Osaka Prefecture University. He has been a Research Fellow of Japan Society for Promotion of Science (JSPS) in Department of Materials Science and Engineering at Hokkaido University (2004-2006) including a visiting researcher in Laboratoire d'Hydrodynamique at École Polytechnique during 2005. He is currently a PostDoctral researcher in Division of Materials Science and Engineering at Hokkaido University. His research interests include: Low-Reynolds-Number Flow, Matched Asymptotic Expansions, Vortex Particle Method and Brownian Movement.

Mitsuo Kurata: He received his Ph.D. in 1979 from Department of Mechanical Engineering at Osaka Prefecture University. He works in Department of Mechanical Engineering, Setsunan University as a professor since 2001. His research interests are drag reduction and non-contacting and suspending support of air cushion pad.

Teruhiko Kida: He received his Ph.D. in 1972 from Department of Mechanical Engineering at University of Osaka Prefecture (present: Osaka Prefecture University). He is Professor Emeritus of Osaka Prefecture University since 2004. His research interests are numerical simulation of the onset of turbulence by a Vortex Method and a transient low Reynolds number flow.

Manabu Iguchi: He received his M.Sc. (Eng.) in Mechanical Engineering in 1973 from Osaka University. He also received his Ph.D. in Mechanical Engineering in 1981 from Osaka University. He works in Division of Materials Science and Engineering, Graduate School of Engineering of Hokkaido University as a professor since 1996. His research interests are transport phenomena in materials processing operations and development of velocimeters for molten metals at high temperatures.